

# Mirror-skin thickness: A possible observable sensitive to the charge symmetry breaking energy density functional

Tomoya Naito (内藤智也)

*RIKEN Interdisciplinary Theoretical and Mathematical Sciences Program (iTHEMS), Wako 351-0198, Japan and  
Department of Physics, Graduate School of Science,  
The University of Tokyo, Tokyo 113-0033, Japan*

Yuto Hijikata (土方佑斗) and Juzo Zenihiro (銭廣十三)

*Department of Physics, Kyoto University, Kyoto 606-8502, Japan and  
RIKEN Nishina Center, Wako 351-0198, Japan*

Gianluca Colò

*Dipartimento di Fisica, Università degli Studi di Milano, Via Celoria 16, 20133 Milano, Italy and  
INFN, Sezione di Milano, Via Celoria 16, 20133 Milano, Italy*

Hiroyuki Sagawa (佐川弘幸)

*Center for Mathematics and Physics, University of Aizu, Aizu-Wakamatsu 965-8560, Japan and  
RIKEN Nishina Center, Wako 351-0198, Japan*

(Dated: March 10, 2025)

We propose a new observable, named the mirror-skin thickness, in order to extract the strength of the charge symmetry breaking (CSB) term in the energy density functional (EDF). The mirror-skin thickness of  $N = 20$  isotones and  $Z = 20$  isotopes is studied by using Hartree-Fock-Bogoliubov (HFB) calculations with various Skyrme EDFs and adding CSB and charge independence breaking (CIB) terms. It is shown that the mirror-skin thickness is sensitive only to the CSB EDF, but hardly depends on either the isospin symmetric part of the nuclear EDF or the CIB term. Therefore, this observable can be used to extract the magnitude of the CSB term in the EDF quantitatively, either from experimental data or *ab initio* calculations. We have studied the accuracy in the mirror-skin thickness that is needed to extract sensible information. Our study may also help to understand the inconsistency between the strength of the phenomenological CSB and that extracted from *ab initio* calculations [Naito *et al.* *Nuovo. Cim. C* **47**, 52 (2024)]. Among possible mirror pairs for experimental study, we propose the mirror-skin thickness between  $^{42}\text{Ca}$  and  $^{42}\text{Ti}$ , which could be accessed in future experiments in RIBF and/or FRIB.

## I. INTRODUCTION

The nuclear interaction has almost a complete isospin symmetry, i.e., the proton-proton, neutron-neutron, and the isospin  $T = 1$  channel of the proton-neutron interactions are almost the same [1–3]. Accordingly, it is known that properties of mirror nuclei are quite similar, while the breaking of isospin symmetry has been paid attention to. A famous example is the so-called Okamoto-Nolen-Schiffer anomaly [4, 5] of the mass difference of mirror nuclei; the Coulomb interaction is not enough to describe the mass difference of mirror nuclei. Many works including Refs. [6–11] have attempted to solve this problem.

One of the possible solutions to solve the anomaly is the inclusion of the isospin symmetry breaking (ISB) terms of the nuclear interaction. They are a small part of the whole, but their contribution to several nuclear properties has been discussed, mainly the masses [10–14] and the isobaric analogue states [15]. The energy difference in the level scheme of mirror nuclei [16, 17], the differences between the electromagnetic transition probabilities [18], as well as the isovector density of  $N = Z$  nuclei [19], have been proposed as signatures of isospin symmetry breaking. Recently, we showed that the ISB terms of the

nuclear interaction also affect the estimation of the slope parameter of the symmetry energy, often called the  $L$  parameter [20, 21]. Note that these effects depend on the strengths of the ISB terms of the nuclear interaction.

The ISB terms can be divided into two classes: the charge symmetry breaking (CSB) and the charge independence breaking (CIB) ones. The CSB term corresponds to the difference between the proton-proton interaction and the neutron-neutron one, while the CIB one corresponds to the difference between the like-particle interaction and the different-particle one, i.e.,

$$V_{\text{CSB}} = V_{nn} - V_{pp}, \quad (1a)$$

$$V_{\text{CIB}} = \frac{V_{pp} + V_{nn}}{2} - V_{pn}^{T=1}. \quad (1b)$$

The CSB interaction originates from the mass difference of protons and neutrons and from the  $\rho$ - $\omega$  and  $\pi$ - $\eta$  mixings in a meson-exchange representation of the nucleon-nucleon interaction [22–27]. In a quantum chromodynamics (QCD) picture, it originates from  $u$ - and  $d$ -quark mass difference and a partial restoration of  $\bar{q}q$  condensation in the nuclear medium [11]. On the other hand, the CIB interaction mainly originates from the mass difference of charged pions and neutral ones [22, 24, 27].

There have been studies on ISB terms using the chiral effective field theory [28–30]. It has been found that the CSB terms give the dominant contribution to the isospin symmetry breaking of ground-state properties of atomic nuclei [21]; thus, hereinafter, we focus on the CSB interaction only.

The nuclear density functional theory (DFT) [31–33] is a powerful tool to calculate nuclear properties of both ground and excited states systematically [34, 35]. The starting point of the DFT calculation is an energy density functional (EDF). To perform the DFT calculation with the ISB terms, it is indispensable to determine an ISB EDF.

There are two ways to determine an EDF: One is referring to *ab initio* calculations and the other is referring to experimental data (phenomenological approach). We have proposed a way to determine the CSB EDF using *ab initio* calculations [36], and using the QCD sum rule [11]. However, the strengths obtained by these works are much smaller than the phenomenological ones. This might be due to the fact that, in the case of *ab initio* calculations, some nuclei display effects that cannot be accounted for so accurately like deformation or continuum effects. It has to be stressed that ISB effects are smaller than other nuclear many-body correlations or, in other words, they might be smaller than the theoretical accuracy of a number of methods that are available so far. While this is not fully clarified and may deserve further study, at the same time, a precise determination of ISB effects by using phenomenological approaches is still indispensable.

References [13–15] proposed ISB EDFs to reproduce various experimental data, while other references give rather different strengths for the ISB terms starting either from *ab initio* or QCD-based approaches. The possible reason of such a deviation may originate from the fact that the ISB terms are quite small compared to the isospin symmetric terms, and most observables also depend on both the isospin symmetric and ISB terms; thus it is difficult to pin down quantitatively the ISB strength. Therefore, it is important to find a physical observable sensitive only to the ISB terms. The status of CSB EDFs is summarized in Ref. [37].

In this paper, we propose a new physical observable called “mirror-skin thickness”, which is basically sensitive to the CSB term only. We introduce the so-called  $C$ -representation of the Skyrme-like CSB interactions, and their effects on the mirror-skin thickness is discussed term by term.

This paper is organized as follows: First, Sec. II gives the definition of the mirror-skin thickness and its estimation using the liquid drop model. Second, Sec. III gives the theoretical framework of the CSB interaction in nuclear DFT. Then, Sec. IV gives calculation results. Finally, Sec. V is devoted to the summary.

## II. MIRROR-SKIN THICKNESS

We propose a new observable called “mirror-skin thickness” and defined by

$$\Delta R_{\text{mirror}}(Z, N) \equiv R_p(Z, N) - R_n(N, Z), \quad (2)$$

where  $R_p$  and  $R_n$  are the proton and neutron root-mean-square radii, respectively. For an atomic nucleus with the proton and neutron numbers  $Z$  and  $N$ , the radius is denoted by  $R_i(Z, N)$  ( $i = p, n$ ), and alternately  $R_i(N, Z)$  is for a nucleus with the proton and neutron numbers  $N$  and  $Z$ . This mirror-skin thickness is exactly zero if neither the Coulomb nor ISB terms of nuclear interaction is considered. It should be noted that the mirror-skin thickness for the  $N = Z$  nuclei is nothing but the proton-skin thickness.

Before we perform numerical calculations, we estimate the mirror-skin thickness using the liquid-drop model proposed by Myers and Świątecki [38]. The proton and neutron root-mean-square radii, respectively, read [38]

$$R_p = \sqrt{\frac{3}{5}} \left[ R - \frac{1}{2}t + \frac{5}{2} \frac{b^2}{R} + \frac{1}{35} \left( \frac{9}{2K_\infty} + \frac{1}{4J} \right) Ze^2 \right], \quad (3a)$$

$$R_n = \sqrt{\frac{3}{5}} \left[ R + \frac{1}{2}t + \frac{5}{2} \frac{b^2}{R} + \frac{1}{35} \left( \frac{9}{2K_\infty} - \frac{1}{4J} \right) Ze^2 \right] \quad (3b)$$

with

$$R = r_0 A^{1/3} (1 + \bar{\epsilon}), \quad (4a)$$

$$t = \frac{3}{2} r_0 \frac{JI - \frac{1}{12} c_1 ZA^{-1/3}}{Q \left( 1 + \frac{9}{4} \frac{J}{Q} A^{-1/3} \right)}, \quad (4b)$$

$$I = \frac{N - Z}{A}, \quad (4c)$$

$$\bar{\epsilon} = \frac{-2a_2 A^{-1/3} + L\bar{\delta}^2 + c_1 Z^2 A^{-4/3}}{K_\infty}, \quad (4d)$$

$$\bar{\delta} = \frac{I + \frac{3}{16} \frac{c_1}{Q} ZA^{-2/3}}{1 + \frac{9}{4} \frac{J}{Q} A^{-1/3}}, \quad (4e)$$

$$c_1 = \frac{3e^2}{5r_0}. \quad (4f)$$

Here,  $J \simeq 30$  MeV [39] is the symmetry energy at the saturation density,  $L$  is the slope of the symmetry energy,  $K_\infty \simeq 226$  MeV [40] is the incompressibility,  $Q \simeq 17$  MeV [38] is the effective surface stiffness coefficient,  $a_2 \simeq 20$  MeV [38] is the surface energy coefficient,  $b \simeq 1$  fm is the surface width [41, 42], and  $r_0 \simeq 1.18$  fm [38]. Note that  $b$  can be different for protons and neutrons, but for simplicity, we approximate that  $b$  for protons is identical to that for neutrons. In Ref. [41], it is confirmed that  $\sqrt{\frac{3}{5}} \frac{5}{2R} (b_n^2 - b_p^2)$  is less than 0.1 fm even in the case of large proton-neutron asymmetry, and

the value is model independent. Hence, this approximation is good enough in the current discussion. It should also be noted that this representation does not include the effect of isospin symmetry breaking other than the Coulomb interaction.

We take the approximation

$$\begin{aligned} \frac{b^2}{R} &= \frac{b^2}{r_0 A^{1/3} (1 + \bar{\varepsilon})} \\ &\simeq \frac{b^2}{r_0 A^{1/3} (1 - \bar{\varepsilon})} \end{aligned} \quad (5)$$

since  $\bar{\delta} \simeq -0.07$  and  $\bar{\varepsilon} \simeq -0.05$  (for  $^{48}\text{Ni}$ ). Then, we obtain

$$R_p(Z, N) \simeq \sqrt{\frac{3}{5}} \left\{ R_0(Z, N) + R_1(Z, N) + \left[ \frac{9}{70K_\infty} + R_2(Z, N) + R_3(Z, N) \right] Ze^2 + R_4(Z, N) Z^2 e^4 \right\}, \quad (6a)$$

$$R_n(Z, N) \simeq \sqrt{\frac{3}{5}} \left\{ R_0(Z, N) - R_1(Z, N) + \left[ \frac{9}{70K_\infty} + R_2(Z, N) - R_3(Z, N) \right] Ze^2 + R_4(Z, N) Z^2 e^4 \right\} \quad (6b)$$

with

$$R_0(Z, N) = r_0 A^{1/3} + \frac{5}{2} \frac{b^2}{r_0 A^{1/3}} - \left( r_0 A^{1/3} - \frac{5}{2} \frac{b^2}{r_0 A^{1/3}} \right) \frac{1}{K_\infty} \left[ 2a_2 A^{-1/3} - \frac{I^2 L}{\left( 1 + \frac{9}{4} \frac{J}{Q} A^{-1/3} \right)^2} \right], \quad (7a)$$

$$R_1(Z, N) = -\frac{3}{4} r_0 \frac{JI}{Q \left( 1 + \frac{9}{4} \frac{J}{Q} A^{-1/3} \right)}, \quad (7b)$$

$$R_2(Z, N) = \frac{1}{K_\infty} \left( r_0 A^{1/3} - \frac{5}{2} \frac{b^2}{r_0 A^{1/3}} \right) \left[ ZA^{-4/3} + \frac{3}{8} \frac{IA^{-2/3}}{\left( 1 + \frac{9}{4} \frac{J}{Q} A^{-1/3} \right)^2} \frac{L}{Q} \right] \frac{3}{5r_0}, \quad (7c)$$

$$R_3(Z, N) = \frac{3}{80} \frac{A^{-1/3}}{Q} + \frac{1}{140J} - \frac{27}{320} \frac{JA^{-2/3}}{\left( 1 + \frac{9}{4} \frac{J}{Q} A^{-1/3} \right)} \frac{1}{Q^2}, \quad (7d)$$

$$R_4(Z, N) = \frac{81}{800} \frac{1}{K_\infty} \frac{L(2r_0^2 A^{2/3} - 5b^2)}{16r_0^3 A^{5/3}} \frac{1}{\left( 1 + \frac{9}{4} \frac{J}{Q} A^{-1/3} \right)^2} \frac{1}{Q^2}, \quad (7e)$$

where  $R_0(Z, N) = R_0(N, Z)$ ,  $R_1(Z, N) = -R_1(N, Z)$ ,  $R_3(Z, N) = R_3(N, Z)$ , and  $R_4(Z, N) = R_4(N, Z)$  hold. Therefore, the mirror-skin thickness in the liquid-drop model reads

$$\begin{aligned} \Delta R_{\text{mirror}}(Z, N) &= R_p(Z, N) - R_n(Z, N) \\ &\simeq \sqrt{\frac{3}{5}} \left\{ R_0(Z, N) + R_1(Z, N) + \left[ \frac{9}{70K_\infty} + R_2(Z, N) + R_3(Z, N) \right] Ze^2 + R_4(Z, N) Z^2 e^4 \right\} \\ &\quad - \sqrt{\frac{3}{5}} \left\{ R_0(N, Z) - R_1(N, Z) + \left[ \frac{9}{70K_\infty} + R_2(N, Z) - R_3(N, Z) \right] Ne^2 + R_4(N, Z) N^2 e^4 \right\} \\ &= \sqrt{\frac{3}{5}} \left\{ (Z - N) \frac{9}{70K_\infty} + [ZR_2(Z, N) - NR_2(N, Z)] + AR_3 + R_4(Z, N) (Z^2 - N^2) e^2 \right\} e^2 \\ &= \sqrt{\frac{3}{5}} \left( (Z - N) \left\{ \frac{9}{70K_\infty} + \frac{1}{K_\infty} \left( r_0 A^{1/3} - \frac{5}{2} \frac{b^2}{r_0 A^{1/3}} \right) \left[ A^{-1/3} - \frac{3}{8} \frac{A^{-2/3}}{\left( 1 + \frac{9}{4} \frac{J}{Q} A^{-1/3} \right)^2} \frac{L}{Q} \right] \frac{3}{5r_0} \right. \right. \\ &\quad \left. \left. + AR_4(Z, N) e^2 \right\} + AR_3(Z, N) \right) e^2. \end{aligned} \quad (8)$$

The mirror-skin thickness is zero if we neglect the Coulomb interaction, i.e.,  $e^2 = 0$ .

For  $^{48}\text{Ni}$ , the mirror-skin thickness in the liquid-drop model [Eq. (8)] reads

$$\begin{aligned} \Delta R_{\text{mirror}}(Z = 28, N = 20) &= 0.0028(Z - N) + 0.00059A \text{ fm} \\ &= 0.051 \text{ fm}, \end{aligned} \quad (9)$$

We can easily find that even in  $N = Z$  nuclei, the mirror-skin thickness, i.e., the proton-skin thickness, has a finite value. The expression for  $\Delta R_{\text{mirror}}$  in the liquid-drop model in Eq. (8) shows that a proton-rich nucleus ( $Z > N$ ) has a larger  $\Delta R_{\text{mirror}}$  than the neutron-rich one. We should also notice that  $\Delta R_{\text{mirror}}$  could be negative for  $N \gg Z$  nuclei, while it will be shown that all the DFT calculation always gives positive  $\Delta R_{\text{mirror}}$ .

### III. THEORETICAL FRAMEWORK

#### A. Calculation setup

We perform Skyrme Hartree-Fock-Bogoliubov (HFB) calculations [33, 43] by assuming the spherical symmetry. The radial wave function is obtained from the HFB

---


$$v_{\text{Sky}}^{\text{CSB}}(\mathbf{r}) = \left\{ s_0(1 + y_0 P_\sigma) \delta(\mathbf{r}) + \frac{s_1}{2}(1 + y_1 P_\sigma) [\mathbf{k}^\dagger \delta(\mathbf{r}) + \delta(\mathbf{r}) \mathbf{k}^2] + s_2(1 + y_2 P_\sigma) \mathbf{k}^\dagger \cdot \delta(\mathbf{r}) \mathbf{k} \right\} \frac{\tau_{z1} + \tau_{z2}}{4}, \quad (10)$$

where  $\mathbf{r} = \mathbf{r}_1 - \mathbf{r}_2$ ,  $\mathbf{R} = (\mathbf{r}_1 + \mathbf{r}_2)/2$ , and  $P_\sigma = (1 + \boldsymbol{\sigma}_1 \cdot \boldsymbol{\sigma}_2)/2$ . Here,  $\tau_{zj}$  is the  $z$ -projection of the isospin operator for the nucleon  $j$  ( $\tau_{zj} = +1$  for neutrons and  $\tau_{zj} = -1$  for protons) and  $\mathbf{k}$  is the operator of the relative momentum. Accordingly the CSB energy density reads [21, 48]

$$\mathcal{E}_{\text{CSB}} = \frac{\tilde{s}_0}{8} (\rho_n^2 - \rho_p^2) + \frac{1}{16} (\tilde{s}_1 + 3\tilde{s}_2) (\rho_n \tau_n - \rho_p \tau_p) - \frac{3}{64} (\tilde{s}_1 - \tilde{s}_2) (\rho_n \Delta \rho_n - \rho_p \Delta \rho_p) - \frac{1}{32} (\tilde{s}_1 - \tilde{s}_2) (\mathbf{J}_n^2 - \mathbf{J}_p^2), \quad (11)$$

where  $\rho$ ,  $\tau$ , and  $\mathbf{J}$  are the particle, kinetic, and spin-orbit densities, respectively. Since the parameters  $s_j$  and  $y_j$  always appear together as  $s_0(1 - y_0)$ ,  $s_1(1 - y_1)$ , and  $s_2(1 + y_2)$ , we define

$$\tilde{s}_0 = s_0(1 - y_0), \quad (12a)$$

$$\tilde{s}_1 = s_1(1 - y_1), \quad (12b)$$

$$\tilde{s}_2 = s_2(1 + y_2). \quad (12c)$$


---

$$\mathcal{E}_{\text{CSB}} = C_{\text{CSB}}^\rho (\rho_n^2 - \rho_p^2) + C_{\text{CSB}}^\tau (\rho_n \tau_n - \rho_p \tau_p) + C_{\text{CSB}}^{\Delta \rho} (\rho_n \Delta \rho_n - \rho_p \Delta \rho_p), \quad (13)$$

where these  $C$ -parameters are given by

$$C_{\text{CSB}}^\rho = \frac{\tilde{s}_0}{8}, \quad (14a)$$

$$C_{\text{CSB}}^\tau = \frac{1}{16} (\tilde{s}_1 + 3\tilde{s}_2), \quad (14b)$$

$$C_{\text{CSB}}^{\Delta \rho} = -\frac{3}{64} (\tilde{s}_1 - \tilde{s}_2). \quad (14c)$$

solution in coordinate space, with a spatial mesh of 0.1 fm and a box size of 16 fm.

The SLy4 EDF [44] and the volume-type pairing interaction [43] are used for the isospin symmetric particle-hole and particle-particle channel, respectively. The Hartree-Fock-Slater approximation, i.e., the local density approximation, is used for the Coulomb interaction [45]. The single-particle orbitals up to 60 MeV in the Hartree-Fock equivalent energy [46] is considered for the HFB calculation and the strength of the pairing interaction ( $-194.2 \text{ MeV fm}^3$ ) is determined to reproduce the neutron pairing gap of  $^{120}\text{Sn}$  as 1.4 MeV [47]. On top of it, the CSB EDF is considered, which will be explained below. Note that the pairing strength is kept even if the ISB interaction is considered.

We focus on  $Z = 20$  isotopes and  $N = 20$  isotones with the mass number  $A = 38, 40, 42, 44, 46$ , and 48 in our numerical study of the mirror-skin thickness since they are proton- or neutron-magic nuclei and thus expected to be spherical.

#### B. Skyrme-type CSB interaction

The Skyrme-type CSB interaction is defined by [13–15, 21, 48]

---

Hereinafter, the  $\mathbf{J}^2$  term is neglected for simplicity, as did in the SLy4 EDF [44].

The so-called the  $C$ -representation of a Skyrme EDF [49] is also widely used. This  $C$ -representation adopts the coupling constants associated with the different types of densities, generalized densities or its gradients, which is convenient in the present context. We define the CSB EDF in the  $C$ -representation as

---

Inversely,  $\tilde{s}_0$ ,  $\tilde{s}_1$ , and  $\tilde{s}_2$  are written as

$$\tilde{s}_0 = 8C_{\text{CSB}}^\rho, \quad (15a)$$

$$\tilde{s}_1 = 4C_{\text{CSB}}^\tau - 16C_{\text{CSB}}^{\Delta \rho}, \quad (15b)$$

$$\tilde{s}_2 = 4C_{\text{CSB}}^\tau + \frac{16}{3}C_{\text{CSB}}^{\Delta \rho}, \quad (15c)$$

respectively.

## IV. CALCULATION RESULTS

### A. EDF dependence of mirror skin

Figure 1 shows the mirror-skin thickness calculated by different Skyrme EDFs: SLy4, SLy5 [44], SAMi [50], SGII [51], SkM\* [52], HFB9 [53], UNEDF0 [54], UNEDF1 [55], and UNEDF2 [56]. These calculations using a variety of EDFs allow estimating the model dependence of the mirror-skin thickness. This is rather small, as shown in Fig. 1; in fact, the variation among different EDFs is about 0.005 fm, except when including the three variants of UNEDF: then, it can arrive at about 0.01 fm.

Moreover, the mirror-skin thickness hardly depends on the symmetry energy. Figure 2 shows the dependence of  $\Delta R_{\text{mirror}}$  on the symmetry energy at saturation  $J$ . All these calculations are performed using the SAMi-J family [57]. The  $J$ -dependence is much weaker than that on the CSB strength, as will be seen in Sec. IV C. In particular, the symmetry energy dependence of the mirror-skin thickness in the  $N = 20$  isotones is negligibly small.

### B. CIB dependence of mirror skin

We also check that the mirror-skin thickness does not depend on the CIB strength. The sensitivity with respect to the leading-order CIB strength ( $u_0$  in the next formula, analogous to the  $t_0$  in the standard Skyrme interaction) is two orders of magnitude smaller than that to the CSB strength, which will be shown later. Therefore, the mirror-skin thickness could be a useful quantity for pinning down the strength of the CSB interaction.

The leading-order Skyrme-like CIB interaction

$$v_{\text{Sky}}^{\text{CIB}}(\mathbf{r}) = \frac{u_0}{2} (1 + z_0 P_\sigma) \delta(\mathbf{r}) \tau_{z1} \tau_{z2} \quad (16)$$

is considered on top of the SLy4 interaction and the volume-type pairing interaction. The CIB strength is varied from  $u_0 = 0$  to  $25 \text{ MeV fm}^3$ , taking  $z_0 = -1$ . The mirror-skin thickness with the different CIB strength is shown in Fig. 3. It is seen that the mirror-skin thickness does not depend on the CIB interaction.

### C. CSB dependence of mirror skin

#### 1. $C_{\text{CSB}}^\rho$ -term dependence

First, we focus on the  $C_{\text{CSB}}^\rho$  term in Eq. (13), which corresponds to the  $s_0$  term in Eq. (11). Here,  $-C_{\text{CSB}}^\rho$  is varied from 0 to  $10 \text{ MeV fm}^3$ , which corresponds to 0 to  $80 \text{ MeV fm}^3$  in  $-\tilde{s}_0$ , considering neither the  $C_{\text{CSB}}^\tau$  nor

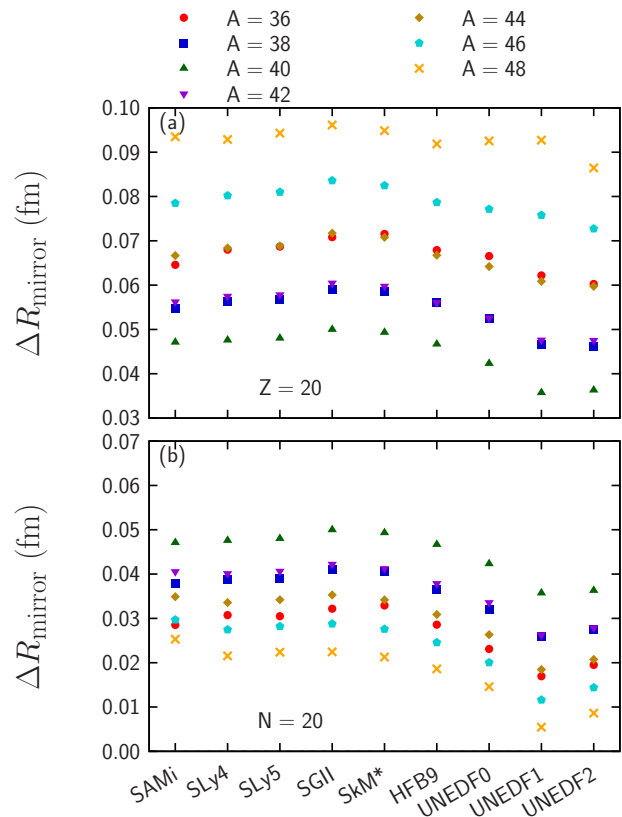


FIG. 1. EDF dependence of the mirror-skin thickness  $\Delta R_{\text{mirror}}$ . The SLy4, SLy5 [44], SAMi [50], SGII [51], SkM\* [52], HFB9 [53], UNEDF0 [54], UNEDF1 [55], and UNEDF2 [56] EDFs and the volume-type pairing interaction [43] are used for the isospin symmetric particle-hole and particle-particle channel, respectively. The Hartree-Fock-Slater approximation, i.e., the local density approximation, is used for the Coulomb interaction [45].

$C_{\text{CSB}}^\Delta$  term. Note that the strongest phenomenological CSB EDF has  $\tilde{s}_0 \simeq -50 \text{ MeV fm}^3$  [37].

Figure 4 shows the  $C_{\text{CSB}}^\rho$  dependence of the mirror-skin thickness  $\Delta R_{\text{mirror}}$ . The  $C_{\text{CSB}}^\rho$  dependence of the mirror-skin thickness is stronger for more proton-rich nuclei, as expected from Eq. (8) in Sec. II. For instance, the slopes of  $^{36}\text{Ca}$  ( $5.4 \times 10^{-3} \text{ MeV}^{-1} \text{ fm}^{-2}$ ) and  $^{48}\text{Ni}$  ( $6.3 \times 10^{-3} \text{ MeV}^{-1} \text{ fm}^{-2}$ ) are almost three times larger than that of  $^{48}\text{Ca}$  ( $2.0 \times 10^{-3} \text{ MeV}^{-1} \text{ fm}^{-2}$ ).

Experimentally, neutron radii can be measured within a 0.5% accuracy; hence, the absolute value of the expected experimental error of  $R_n$  is about 0.02 fm. Proton radii can be extracted from charge radii, which can be measured more accurately. Therefore, the absolute value of the experimental error of  $\Delta R_{\text{mirror}}$  can be about 0.02 fm and accordingly, the absolute error of  $C_{\text{CSB}}^\rho$  can be  $6.0 \text{ MeV fm}^3$  using  $^{42}\text{Ca}$ .

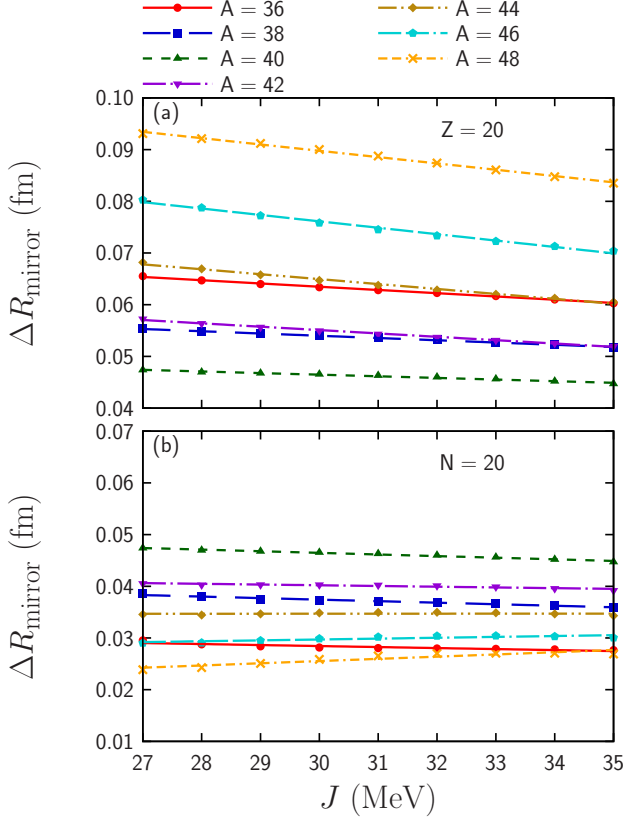


FIG. 2. Mirror-skin thickness  $\Delta R_{\text{mirror}}$  as functions of the symmetry energy at the saturation density  $J$ . The SAMi-J family [57] and the volume-type pairing interaction [43] are used for the isospin symmetric particle-hole and particle-particle channel, respectively. The Hartree-Fock-Slater approximation, i.e., the local density approximation, is used for the Coulomb interaction [45].

## 2. $C_{\text{CSB}}^{\tau}$ - and $C_{\text{CSB}}^{\Delta\rho}$ -term dependence

Next, we discuss the  $C_{\text{CSB}}^{\tau}$  and  $C_{\text{CSB}}^{\Delta\rho}$  dependences of  $\Delta R_{\text{mirror}}$ . To determine the range of  $C_{\text{CSB}}^{\tau}$ , we compare the contributions to the equation of state by the  $C_{\text{CSB}}^{\rho}$  term and by the  $C_{\text{CSB}}^{\tau}$  term. Note that the  $C_{\text{CSB}}^{\Delta\rho}$  term does not contribute to the equation of state. The CSB contribution to the equation of state reads

$$\frac{E_{\text{CSB}}}{A} = C_{\text{CSB}}^{\rho} \rho + \frac{4}{5} \left( \frac{3\pi^2}{2} \right)^{2/3} C_{\text{CSB}}^{\tau} \rho^{5/3}. \quad (17)$$

Therefore, the  $C_{\text{CSB}}^{\rho}$ -term contribution to the equation of state at the saturation density  $\rho_0$  is equivalent to the  $C_{\text{CSB}}^{\tau}$ -term under the assumption

$$C_{\text{CSB}}^{\tau} = \frac{5}{4} \left( \frac{3\pi^2}{2} \right)^{-2/3} C_{\text{CSB}}^{\rho} \rho_0^{-2/3}. \quad (18)$$

For instance,  $C_{\text{CSB}}^{\rho} \simeq -10 \text{ MeV fm}^3$  corresponds to  $C_{\text{CSB}}^{\tau} \simeq -7.0 \text{ MeV fm}^5$  as far as the EoS contribution is

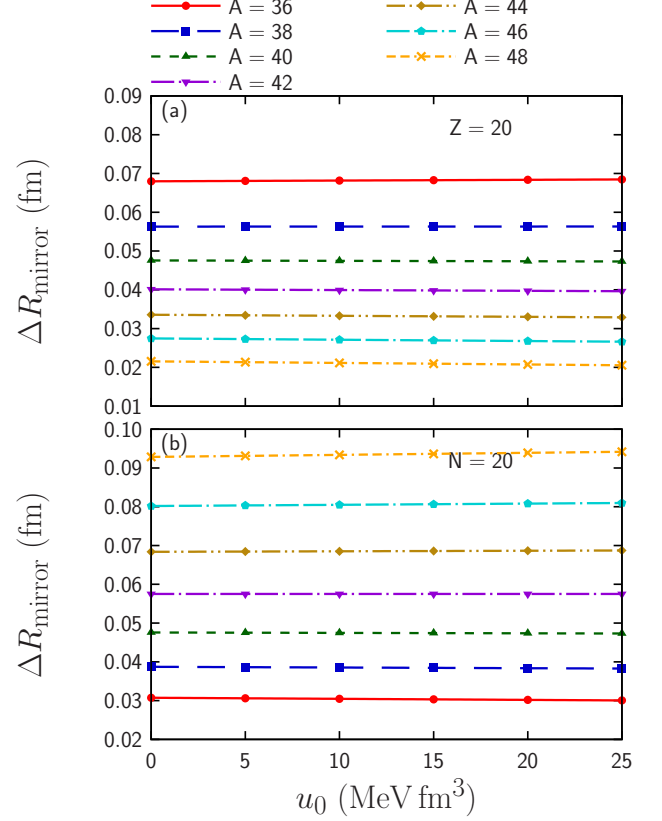


FIG. 3. Mirror-skin thickness  $\Delta R_{\text{mirror}}$  as functions of the CIB strength  $u_0$ . The SLy4 EDF [44] and the volume-type pairing interaction [43] are used for the isospin symmetric particle-hole and particle-particle channel, respectively. The Hartree-Fock-Slater approximation, i.e., the local density approximation, is used for the Coulomb interaction [45].

concerned. Considering this relation, we vary  $C_{\text{CSB}}^{\tau}$  from 0 to  $-10 \text{ MeV fm}^5$ . In contrast,  $C_{\text{CSB}}^{\Delta\rho}$  can be both negative and positive because  $\Delta\rho(\mathbf{r})$  can be both negative and positive, in contrast to  $C_{\text{CSB}}^{\rho}$  and  $C_{\text{CSB}}^{\tau}$  dependences; therefore, we vary  $C_{\text{CSB}}^{\Delta\rho}$  from  $-5$  to  $5 \text{ MeV fm}^5$ .

Figures 5 and 6, respectively, show  $C_{\text{CSB}}^{\tau}$  and  $C_{\text{CSB}}^{\Delta\rho}$  the dependences of  $\Delta R_{\text{mirror}}$ . It is clearly seen that the  $C_{\text{CSB}}^{\tau}$  dependence is much stronger than the  $C_{\text{CSB}}^{\Delta\rho}$  dependence in most cases. In contrast, the  $C_{\text{CSB}}^{\tau}$  dependence is similar to the  $C_{\text{CSB}}^{\rho}$  one.

To understand the reason why the  $C_{\text{CSB}}^{\tau}$  dependence is the strongest, we choose the pair of mirror nuclei  $^{42}\text{Ca}$  and  $^{42}\text{Ti}$  as an example. Hereinafter, for simplicity, the specific CSB interaction with  $C_{\text{CSB}}^{\rho} = -5 \text{ MeV fm}^3$  only ( $C_{\text{CSB}}^{\tau} = -5 \text{ MeV fm}^5$  only or  $C_{\text{CSB}}^{\Delta\rho} = +5 \text{ MeV fm}^5$  only) is referred to as  $C_{\text{CSB}}^{\rho}$ -CSB ( $C_{\text{CSB}}^{\tau}$ -CSB or  $C_{\text{CSB}}^{\Delta\rho}$ -CSB). The results are summarized in Table I.

First, we shall focus on  $^{42}\text{Ca}$ . Figures 7–9 show the CSB potential  $V_{\text{CSB}}$  and the CSB energy density  $4\pi r^2 \mathcal{E}_{\text{CSB}}$  for  $^{42}\text{Ca}$  with the  $C_{\text{CSB}}^{\rho}$ -CSB,  $C_{\text{CSB}}^{\tau}$ -CSB, and

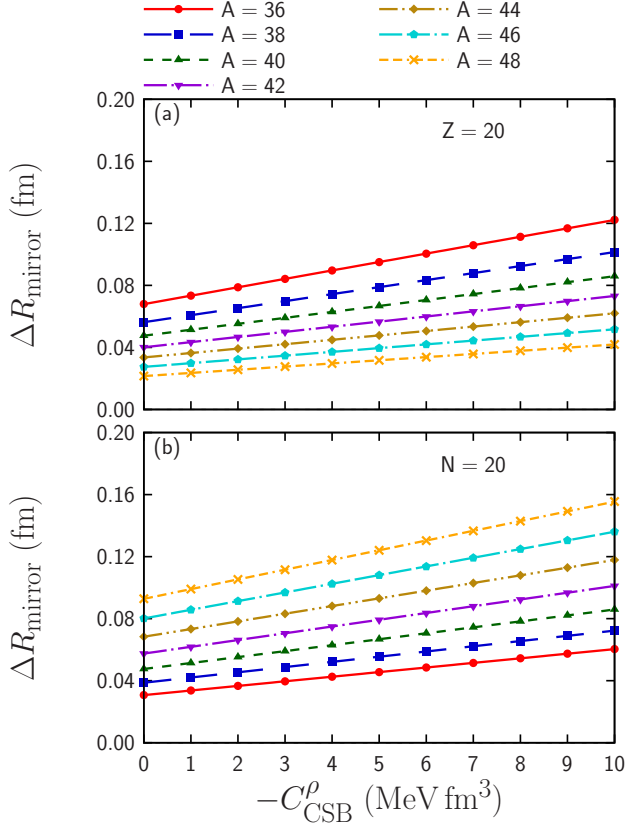


FIG. 4. Mirror-skin thickness  $\Delta R_{\text{mirror}}$  as functions of the CSB strength  $C_{\text{CSB}}^{\rho}$ . The SLy4 EDF [44] and the volume-type pairing interaction [43] are used for the isospin symmetric particle-hole and particle-particle channel, respectively. The Hartree-Fock-Slater approximation, i.e., the local density approximation, is used for the Coulomb interaction [45]. On top of it, the  $C_{\text{CSB}}^{\rho}$  term is considered.

$C_{\text{CSB}}^{\Delta\rho}$ -CSB interactions. The CSB energy density in the  $C$ -parametrization is given in Eq. (13), and the CSB effective mean-field potentials for protons and neutrons, respectively, read

$$V_{\text{CSB}}^p(\mathbf{r}) = \frac{\partial \mathcal{E}_{\text{CSB}}}{\delta \rho_p} = - \left[ 2C_{\text{CSB}}^{\rho} \rho_p(\mathbf{r}) + C_{\text{CSB}}^{\tau} \tau_p(\mathbf{r}) + 2C_{\text{CSB}}^{\Delta\rho} \Delta \rho_p(\mathbf{r}) \right], \quad (19a)$$

$$V_{\text{CSB}}^n(\mathbf{r}) = \frac{\partial \mathcal{E}_{\text{CSB}}}{\delta \rho_n} = + \left[ 2C_{\text{CSB}}^{\rho} \rho_n(\mathbf{r}) + C_{\text{CSB}}^{\tau} \tau_n(\mathbf{r}) + 2C_{\text{CSB}}^{\Delta\rho} \Delta \rho_n(\mathbf{r}) \right] \quad (19b)$$

As seen in Eq. (19), the CSB potential induced by the  $C_{\text{CSB}}^{\rho}$ -CSB interaction is proportional to the proton or neutron density,  $\rho_p$  or  $\rho_n$ , and affects the whole  $\rho_p$  and  $\rho_n$  (see Fig. 10). Eventually,  $\Delta R_{\text{mirror}}$  increases by about 40%. Since  $V_{\text{CSB}}$  for the neutrons is attractive,

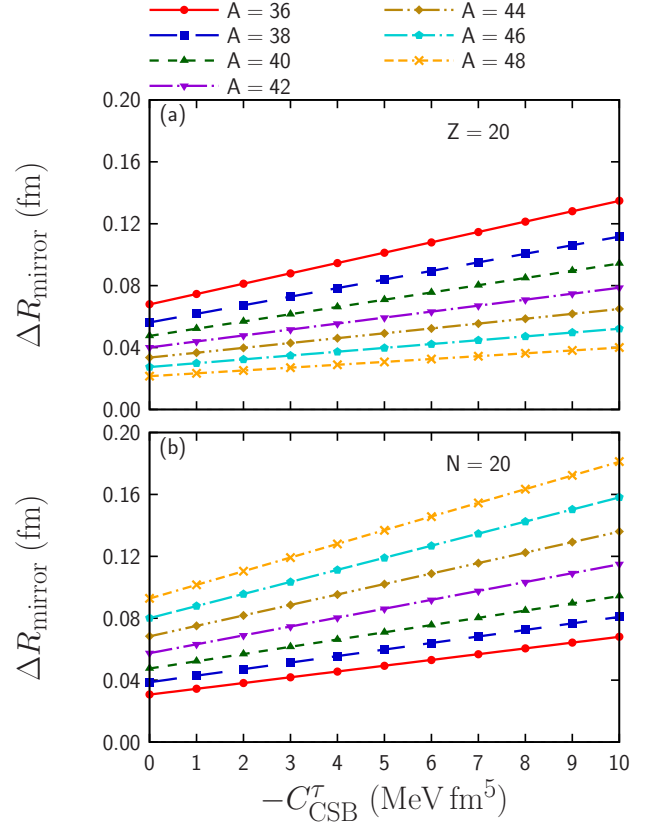


FIG. 5. Same as Fig. 4 but for the  $C_{\text{CSB}}^{\tau}$  dependence.

$\rho_n$  shrinks and since  $V_{\text{CSB}}$  for the protons is repulsive,  $\rho_p$  extend. In total,  $\mathcal{E}_{\text{CSB}}(r)r^2$  is always negative, and thus,  $E_{\text{CSB}}$  is also negative.

The  $C_{\text{CSB}}^{\tau}$ -CSB interaction shows a similar behavior as the  $C_{\text{CSB}}^{\rho}$ -CSB one. The  $C_{\text{CSB}}^{\tau}$ -CSB potential is proportional to the kinetic density,  $\tau_p$  or  $\tau_n$ , and accordingly, it also affects the whole radial dependence  $\rho_p$  and  $\rho_n$  (see Fig. 11). Compared to the  $C_{\text{CSB}}^{\rho}$ -CSB potential, the  $C_{\text{CSB}}^{\tau}$ -CSB potential is weak; however, the total effect is slightly larger due to the effective mass. Indeed, the  $C_{\text{CSB}}^{\tau}$ -CSB interaction contributes to the effective mass as

$$\frac{\hbar^2}{2m_{\text{CSB}}^{*p}(\mathbf{r})} = -C_{\text{CSB}}^{\tau} \rho_p(\mathbf{r}), \quad (20a)$$

$$\frac{\hbar^2}{2m_{\text{CSB}}^{*n}(\mathbf{r})} = +C_{\text{CSB}}^{\tau} \rho_n(\mathbf{r}). \quad (20b)$$

In the case of  $C_{\text{CSB}}^{\tau} < 0$ , the proton effective mass becomes lighter, while the neutron one becomes heavier. Thus, proton radii increase and neutron radii shrink; accordingly, the mirror-skin thickness becomes larger due to the change in the effective mass. The change of  $\hbar^2/2m^*$  is about  $0.5 \text{ MeV fm}^2$  for  $C_{\text{CSB}}^{\tau} = -5 \text{ MeV fm}^5$ , which is 2.5% of the bare mass contribution. The energy density  $\mathcal{E}_{\text{CSB}}(r)r^2$  also behaves similarly to the  $C_{\text{CSB}}^{\rho}$ -CSB interaction, while the absolute value is slightly

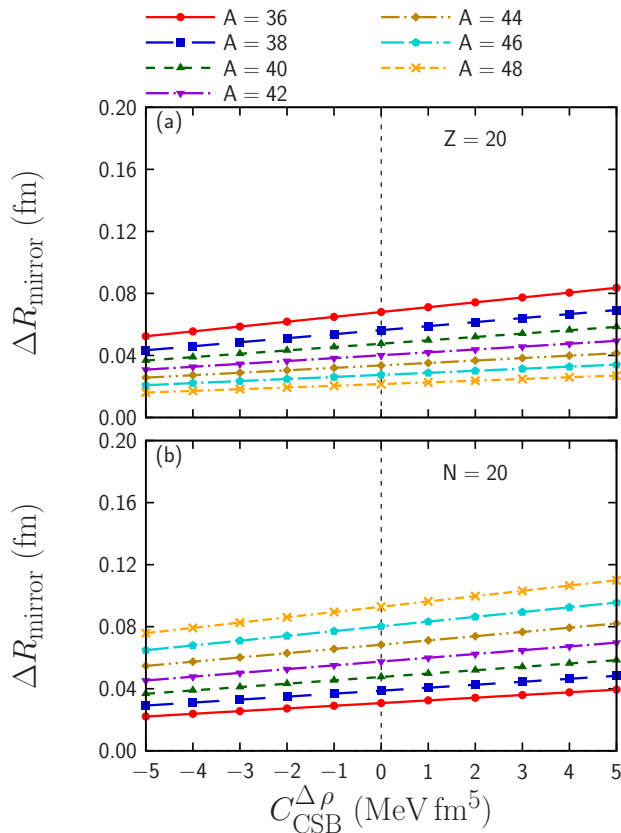


FIG. 6. Same as Fig. 4 but for the  $C_{\text{CSB}}^{\Delta\rho}$  dependence.

larger and accordingly the absolute value of  $E_{\text{CSB}}$  and the CSB effect on  $\Delta R_{\text{mirror}}$  are also larger by about 20%.

In contrast, the  $C_{\text{CSB}}^{\Delta\rho}$ -CSB interaction behaves differently from the other two CSB interactions. The  $C_{\text{CSB}}^{\Delta\rho}$ -CSB potential is proportional to  $\Delta\rho_p$  or  $\Delta\rho_n$ ; accordingly it has an oscillating structure. Thus, the net change of  $\rho_p$  and  $\rho_n$  is smaller than in the case of the other two CSB interactions (see Fig. 12). The energy density  $\mathcal{E}_{\text{CSB}}(r)r^2$  also oscillates and, accordingly, the absolute value of  $E_{\text{CSB}}$  and the CSB effect of  $\Delta R_{\text{mirror}}$  are the smallest.

Next, we compare the result of  $^{42}\text{Ti}$  to that of  $^{42}\text{Ca}$ . Here, we take the  $C_{\text{CSB}}^{\rho}$ -CSB interaction as an example. Figure 13 shows the  $C_{\text{CSB}}^{\rho}$ -CSB potential and the energy density. The CSB mean-field potential for  $^{42}\text{Ti}$  has a quite similar behavior to that for  $^{42}\text{Ca}$ ; and accordingly, the changes of  $R_p$  and  $R_n$  for  $^{42}\text{Ti}$  are almost the same size as those for  $^{42}\text{Ca}$ . However, the energy density almost vanishes in the internal region, and accordingly, the absolute value of  $E_{\text{CSB}}$  of  $^{42}\text{Ti}$  is smaller than that of  $^{42}\text{Ca}$ . This difference is basically due to the Coulomb interaction. Without the Coulomb interaction,  $\rho_p(r)$  is smaller than  $\rho_n(r)$  for  $^{42}\text{Ca}$ . Due to the Coulomb interaction,  $\rho_p$  expands, and accordingly,  $\rho_n^2 - \rho_p^2$  is always positive. In contrast, for  $^{42}\text{Ti}$ , without the Coulomb interaction,  $\rho_p(r)$  is basically larger than  $\rho_n(r)$ . Due to

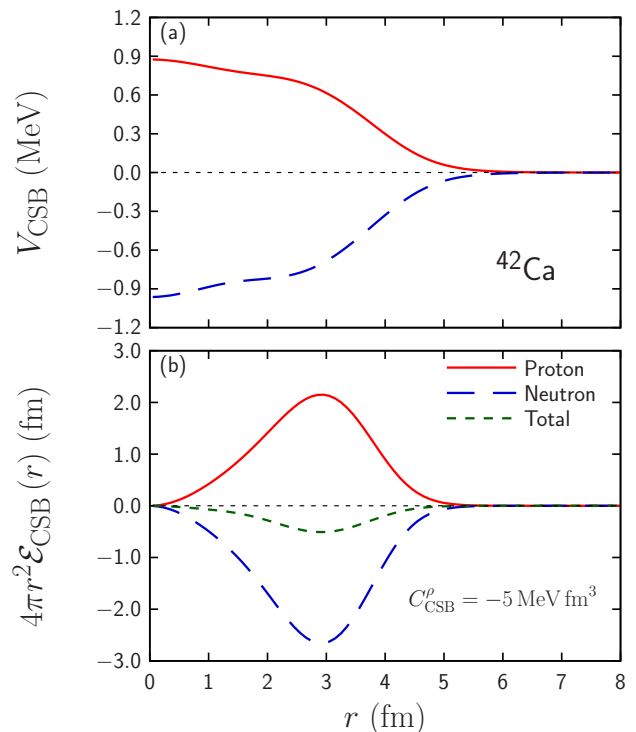


FIG. 7. (a) CSB potential and (b) the integrand of the CSB energy density of  $^{42}\text{Ca}$ , as functions of  $r$ , for  $C_{\text{CSB}}^{\rho} = -5 \text{ MeV fm}^3$ .

the Coulomb interaction,  $\rho_p$  extends, and accordingly,  $\rho_n^2 - \rho_p^2$  in the internal region reaches to zero.

If we assume the accuracy of  $\Delta R_{\text{mirror}}$  is about 0.02 fm, the absolute error of  $C_{\text{CSB}}^{\tau}$  and  $C_{\text{CSB}}^{\Delta\rho}$  can be, respectively, 5.2 and 10.8  $\text{MeV fm}^3$  using  $^{42}\text{Ca}$ .

## V. SUMMARY

In this paper, we proposed a new observable, named the mirror-skin thickness  $\Delta R_{\text{mirror}}$ , to pin down the magnitude of the CSB term in the nuclear EDF. As examples, we studied the mirror-skin thickness of  $N = 20$  isotones and  $Z = 20$  isotopes by using HFB calculations with various Skyrme EDFs and adding CSB and CIB terms. It is shown that the mirror-skin thickness is sensitive only to the CSB EDF, but hardly depends on either the isospin symmetric part of the nuclear interaction or the CIB term. Therefore, this observable can be used to determine the CSB EDF quantitatively either from experimental data or *ab initio* calculation.

The  $\rho^2$  and  $\rho\tau$  terms of the CSB EDF give similar substantial contributions to  $\Delta R_{\text{mirror}}$ , while the  $\rho\Delta\rho$  one gives the smallest contribution. Therefore, it is possible to extract the values of  $C_{\text{CSB}}^{\rho}$  or  $C_{\text{CSB}}^{\tau}$ , namely the coupling constants of the  $\rho^2$  and the  $\rho\tau$  terms, using experimental information on the mirror-skin thickness, while it is difficult to obtain the  $C_{\text{CSB}}^{\Delta\rho}$  value. Among



TABLE I. Total energy,  $E_{\text{tot}}$ , the CSB energy,  $E_{\text{CSB}}$ , proton and neutron root-mean-square radii,  $R_p$  and  $R_n$ , and the mirror-skin thickness  $\Delta R_{\text{mirror}}$  for  $^{42}\text{Ca}$  and  $^{42}\text{Ti}$  calculated with several ISB parameters and the SLy4 interaction. The total energy and the CSB one are shown in MeV and the others are in fm.

ISB			$^{42}\text{Ca}$					$^{42}\text{Ti}$				
$C_{\text{CSB}}^p$	$C_{\text{CSB}}^\tau$	$C_{\text{CSB}}^{\Delta\rho}$	$E_{\text{tot}}$	$E_{\text{CSB}}$	$R_p$	$R_n$	$\Delta R_{\text{mirror}}$	$E_{\text{tot}}$	$E_{\text{CSB}}$	$R_p$	$R_n$	$\Delta R_{\text{mirror}}$
0	0	0	-364.5843	+0.0000	3.4240	3.4369	0.0401	-350.2891	+0.0000	3.4944	3.3838	0.0575
-5	0	0	-365.6038	-1.0596	3.4320	3.4260	0.0566	-349.7843	+0.4587	3.5053	3.3754	0.0793
0	-5	0	-365.8122	-1.3014	3.4328	3.4219	0.0593	-349.7819	+0.4215	3.5080	3.3734	0.0861
0	0	+5	-364.9563	-0.3949	3.4284	3.4306	0.0494	-350.1905	+0.0748	3.5003	3.3789	0.0697

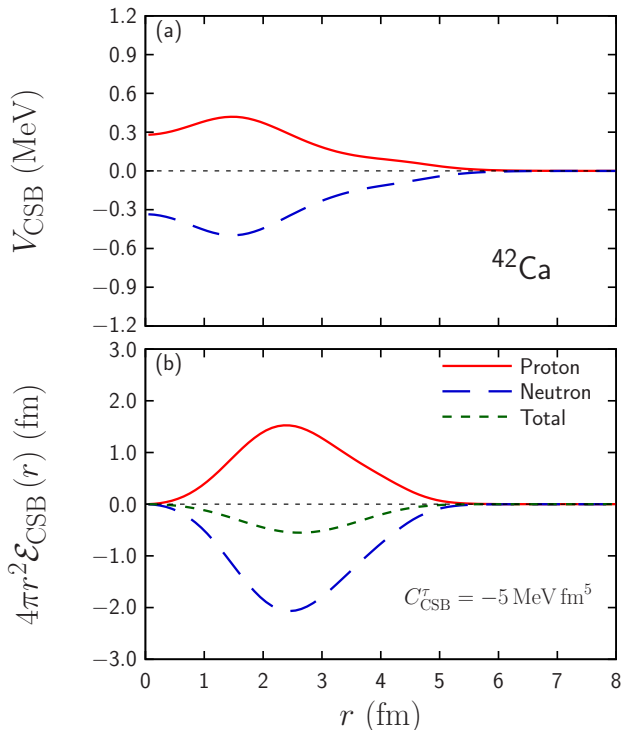


FIG. 8. Same as Fig. 9 but for  $C_{\text{CSB}}^\tau = -5 \text{ MeV fm}^5$ .

the mirror pairs, we propose the experimental study of the mirror-skin thickness between  $^{42}\text{Ca}$  and  $^{42}\text{Ti}$ , or even more exotic pairs of mirror nuclei, which could be accessed in future experiments at RIBF and/or FRIB. The current accuracy on measurement of neutron radii could be enough to extract the information on the CSB interaction, while more accurate measurement and the measurement of density profiles can provide more accurate determination of the coupling constants.

As far as the present study and several previous studies in the literature [13, 14, 20, 21] are concerned, the CSB interaction always gives stronger contribution to most observables than the CIB interaction. Thus, it is an important future perspective to find observables that are equally sensitive, or more sensitive, to the CIB interac-

tion than to the CSB interaction.

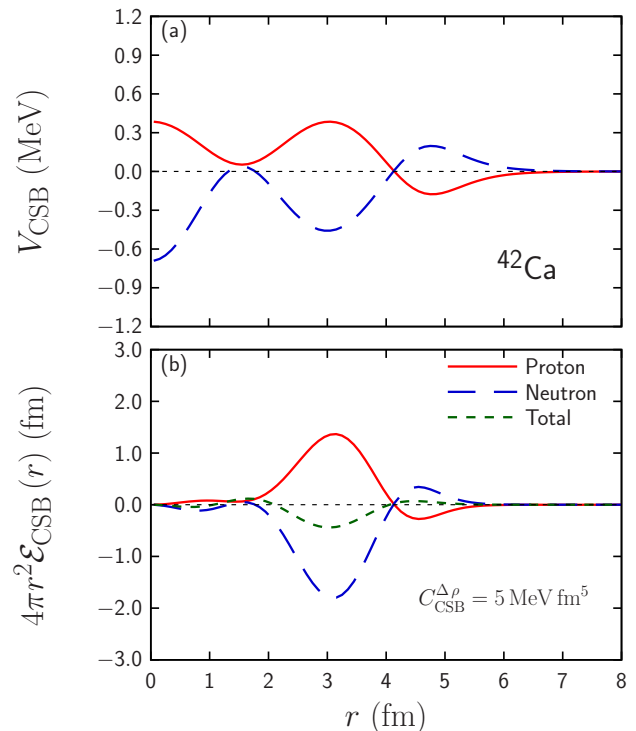


FIG. 9. Same as Fig. 9 but for  $C_{\text{CSB}}^{\Delta\rho} = 5 \text{ MeV fm}^5$ .

## ACKNOWLEDGMENTS

T. N. acknowledges the RIKEN Special Postdoctoral Researcher Program, the JSPS Grant-in-Aid for Research Activity Start-up under Grant No. JP22K20372, the JSPS Grant-in-Aid for Transformative Research Areas (A) under Grant No. JP23H04526, the JSPS Grant-in-Aid for Scientific Research (B) under Grant Nos. JP23H01845 and JP23K26538, the JSPS Grant-in-Aid for Scientific Research (C) under Grant No. JP23K03426, and the JSPS Grant-in-Aid for Early-Career Scientists under Grant No. JP24K17057. The numerical calculations were performed on cluster computers at the RIKEN iTHEMS program.

[1] W. Heisenberg, Über den Bau der Atomkerne. I, Z. Phys. **77**, 1 (1932).

[2] B. Cassen and E. U. Condon, On Nuclear Forces, Phys.

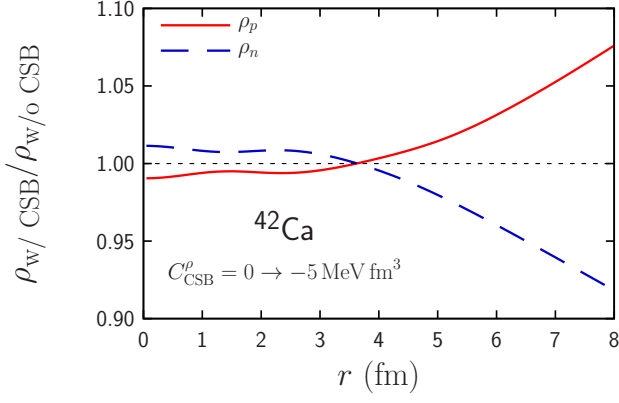


FIG. 10. Ratio between the proton and neutron densities of  $^{42}\text{Ca}$ ,  $\rho_p$  and  $\rho_n$ , without the CSB interaction and those with the CSB interaction ( $C_{\text{CSB}}^\rho = -5 \text{ MeV fm}^3$ ).

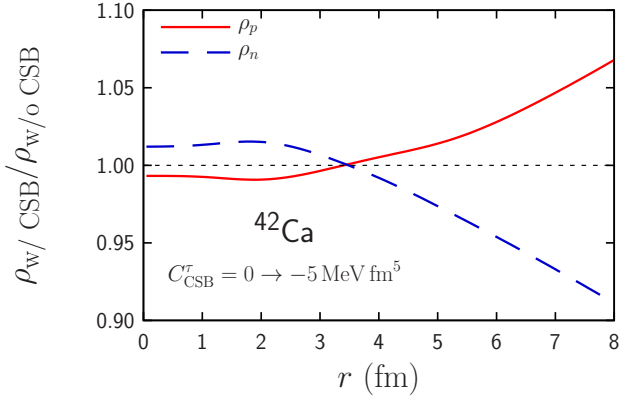


FIG. 11. Same as Fig. 10 but for  $C_{\text{CSB}}^\tau = -5 \text{ MeV fm}^5$ .

Rev. **50**, 846 (1936).

- [3] E. Wigner, On the Consequences of the Symmetry of the Nuclear Hamiltonian on the Spectroscopy of Nuclei, Phys. Rev. **51**, 106 (1937).
- [4] K. Okamoto, Coulomb energy of  $\text{He}^3$  and possible charge asymmetry of nuclear forces, Phys. Lett. **11**, 150 (1964).
- [5] J. A. Nolen, Jr. and J. P. Schiffer, Coulomb Energies, Annu. Rev. Nucl. Sci. **19**, 471 (1969).
- [6] T. Hatsuda, H. Høgaasen, and M. Prakash, QCD sum rules in medium and the Okamoto-Nolen-Schiffer anomaly, Phys. Rev. Lett. **66**, 2851 (1991).
- [7] N. Auerbach, Comment on QCD effects in the nuclear medium, the effective nucleon mass and the Nolen-Schiffer anomaly, Phys. Lett. B **282**, 263 (1992).
- [8] T. Suzuki, H. Sagawa, and A. Arima, Effects of valence nucleon orbits and charge symmetry breaking interaction on the Nolen-Schiffer anomaly of mirror nuclei, Nucl. Phys. A **536**, 141 (1992).
- [9] K. Saito and A. W. Thomas, The Nolen-Schiffer anomaly and isospin symmetry breaking in nuclear matter, Phys. Lett. B **335**, 17 (1994).
- [10] J. M. Dong, Y. H. Zhang, W. Zuo, J. Z. Gu, L. J. Wang, and Y. Sun, Generalized isobaric multiplet mass equation and its application to the Nolen-Schiffer anomaly, Phys.

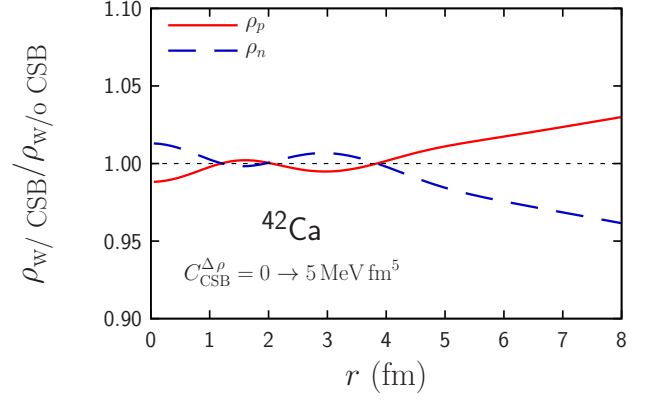


FIG. 12. Same as Fig. 10 but for  $C_{\text{CSB}}^{\Delta\rho} = 5 \text{ MeV fm}^5$ .

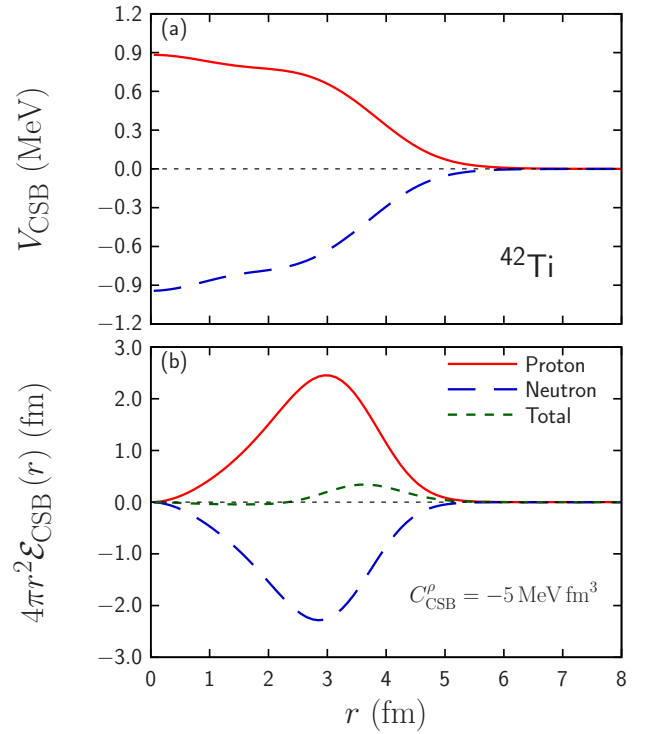


FIG. 13. Same as Fig. 10 but for  $^{42}\text{Ti}$ .

Rev. C **97**, 021301 (2018).

- [11] H. Sagawa, T. Naito, X. Roca-Maza, and T. Hatsuda, QCD-based charge symmetry breaking interaction and the Okamoto-Nolen-Schiffer anomaly, Phys. Rev. C **109**, L011302 (2024).
- [12] P. Bączyk, J. Dobaczewski, M. Konieczka, and W. Satuła, Strong-interaction Isospin-symmetry Breaking within the Density Functional Theory, Acta Phys. Pol. B, Proc. Suppl. **8**, 539 (2016).
- [13] P. Bączyk, J. Dobaczewski, M. Konieczka, W. Satuła, T. Nakatsukasa, and K. Sato, Isospin-symmetry breaking in masses of  $N \simeq Z$  nuclei, Phys. Lett. B **778**, 178 (2018).
- [14] P. Bączyk, W. Satuła, J. Dobaczewski, and M. Konieczka, Isobaric multiplet mass equation within

- nuclear density functional theory, *J. Phys. G* **46**, 03LT01 (2019).
- [15] X. Roca-Maza, G. Colò, and H. Sagawa, Nuclear Symmetry Energy and the Breaking of the Isospin Symmetry: How Do They Reconcile with Each Other?, *Phys. Rev. Lett.* **120**, 202501 (2018).
- [16] D. E. M. Hoff, A. M. Rogers, S. M. Wang, P. C. Bender, K. Brandenburg, K. Childers, J. A. Clark, A. C. Dombos, E. R. Doucet, S. Jin, R. Lewis, S. N. Liddick, C. J. Lister, Z. Meisel, C. Morse, W. Nazarewicz, H. Schatz, K. Schmidt, D. Soltesz, S. K. Subedi, and S. Waniganeththi, Mirror-symmetry violation in bound nuclear ground states, *Nature* **580**, 52 (2020).
- [17] A. Algora, A. Vitéz-Sveicz, A. Poves, G. G. Kiss, B. Rubio, G. de Angelis, F. Recchia, S. Nishimura, T. Rodriguez, P. Sarriguren, J. Agramunt, V. Guadilla, A. Montaner-Pizá, A. I. Morales, S. E. A. Orrigo, D. Napoli, S. M. Lenzi, A. Boso, V. H. Phong, J. Wu, P.-A. Söderström, T. Sumikama, H. Suzuki, H. Takeda, D. S. Ahn, H. Baba, P. Doornenbal, N. Fukuda, N. Inabe, T. Isobe, T. Kubo, S. Kubono, H. Sakurai, Y. Shimizu, S. Chen, B. Blank, P. Ascher, M. Gerbaux, T. Goigoux, J. Giovinazzo, S. Grévy, T. Kurtukián Nieto, C. Margron, W. Gelletly, Z. Dombrádi, Y. Fujita, M. Tanaka, P. Aguilera, F. Molina, J. Eberth, F. Diel, D. Lubos, C. Borcea, E. Ganioglu, D. Nishimura, H. Oikawa, Y. Takei, S. Yagi, W. Kortzen, G. de France, P. Davies, J. Liu, J. Lee, T. Lokotko, I. Kojouharov, N. Kurz, H. Schaffner, and A. Kruppa, Isospin breaking in the  $^{71}\text{Kr}$  and  $^{71}\text{Br}$  mirror system, arXiv:2411.00509 [nucl-ex] (2024).
- [18] K. Wimmer, W. Kortzen, P. Doornenbal, T. Arici, P. Aguilera, A. Algora, T. Ando, H. Baba, B. Blank, A. Boso, S. Chen, A. Corsi, P. Davies, G. de Angelis, G. de France, J.-P. Delaroche, D. T. Doherty, J. Gerl, R. Gernhäuser, M. Girod, D. Jenkins, S. Koyama, T. Motobayashi, S. Nagamine, M. Niikura, A. Obertelli, J. Libert, D. Lubos, T. R. Rodríguez, B. Rubio, E. Sahin, T. Y. Saito, H. Sakurai, L. Sinclair, D. Steppenbeck, R. Taniuchi, R. Wadsworth, and M. Zielinska, Shape Changes in the Mirror Nuclei  $^{70}\text{Kr}$  and  $^{70}\text{Se}$ , *Phys. Rev. Lett.* **126**, 072501 (2021).
- [19] H. Sagawa, S. Yoshida, T. Naito, T. Uesaka, J. Zenihiro, J. Tanaka, and T. Suzuki, Isovector density and isospin impurity in  $^{40}\text{Ca}$ , *Phys. Lett. B* **829**, 137072 (2022).
- [20] T. Naito, X. Roca-Maza, G. Colò, H. Liang, and H. Sagawa, Isospin symmetry breaking in the charge radius difference of mirror nuclei, *Phys. Rev. C* **106**, L061306 (2022).
- [21] T. Naito, G. Colò, H. Liang, X. Roca-Maza, and H. Sagawa, Effects of Coulomb and isospin symmetry breaking interactions on neutron-skin thickness, *Phys. Rev. C* **107**, 064302 (2023).
- [22] E. M. Henley, Charge independence and charge symmetry of nuclear forces, in *Isospin in Nuclear Physics*, edited by D. H. Wilkinson (North-Holland, Amsterdam, 1969) Chap. 2, p. 15.
- [23] S. A. Coon, M. D. Scadron, and P. C. McNamee, On the sign of the  $\rho$ - $\omega$  mixing charge asymmetric  $nn$  potential, *Nucl. Phys. A* **287**, 381 (1977).
- [24] E. M. Henley and G. A. Miller, Meson theory of charge-dependent nuclear forces, in *Mesons in Nuclei, Volume I*, edited by M. Rho and D. Wilkinson (North-Holland, Amsterdam, New York, Oxford, 1979) Chap. 10, p. 405.
- [25] S. A. Coon and M. D. Scadron, Role of  $\pi^0\eta'$  mixing in nuclear charge asymmetry, *Phys. Rev. C* **26**, 562 (1982).
- [26] S. A. Coon and R. C. Barrett,  $\rho$ - $\omega$  mixing in nuclear charge asymmetry, *Phys. Rev. C* **36**, 2189 (1987).
- [27] G. A. Miller, B. M. K. Nefkens, and I. Šlaus, Charge symmetry, quarks and mesons, *Phys. Rep.* **194**, 1 (1990).
- [28] U. van Kolck, J. L. Friar, and T. Goldman, Phenomenological aspects of isospin violation in the nuclear force, *Phys. Lett. B* **371**, 169 (1996).
- [29] J. L. Friar and U. van Kolck, Charge-independence breaking in the two-pion-exchange nucleon-nucleon force, *Phys. Rev. C* **60**, 034006 (1999).
- [30] U. van Kolck, Nuclear Effective Field Theories: Reverberations of the Early Days, *Few-Body Syst.* **62**, 85 (2021).
- [31] P. Hohenberg and W. Kohn, Inhomogeneous Electron Gas, *Phys. Rev.* **136**, B864 (1964).
- [32] W. Kohn and L. J. Sham, Self-Consistent Equations Including Exchange and Correlation Effects, *Phys. Rev.* **140**, A1133 (1965).
- [33] D. Vautherin and D. M. Brink, Hartree-Fock Calculations with Skyrme's Interaction. I. Spherical Nuclei, *Phys. Rev. C* **5**, 626 (1972).
- [34] S. Bogner, A. Bulgac, J. Carlson, J. Engel, G. Fann, R. J. Furnstahl, S. Gandolfi, G. Hagen, M. Horoi, C. Johnson, M. Kortelainen, E. Lusk, P. Maris, H. Nam, P. Navrátil, W. Nazarewicz, E. Ng, G. P. A. Nobre, E. Ormand, T. Papenbrock, J. Pei, S. C. Pieper, S. Quaglioni, K. J. Roche, J. Sarich, N. Schunck, M. Sosonkina, J. Terasaki, I. Thompson, J. P. Vary, and S. M. Wild, Computational nuclear quantum many-body problem: The UN-EDF project, *Comput. Phys. Commun.* **184**, 2235 (2013).
- [35] G. Colò, Nuclear density functional theory, *Adv. Phys.:X* **5**, 1740061 (2020).
- [36] T. Naito, G. Colò, H. Liang, X. Roca-Maza, and H. Sagawa, Toward *ab initio* charge symmetry breaking in nuclear energy density functionals, *Phys. Rev. C* **105**, L021304 (2022).
- [37] T. Naito, G. Colò, T. Hatsuda, H. Liang, X. Roca-Maza, and H. Sagawa, Possible inconsistency between phenomenological and theoretical determinations of charge symmetry breaking in nuclear energy density functionals, *Nuovo Cim. C* **47**, 52 (2024).
- [38] W. D. Myers and W. J. Swiatecki, Droplet-model theory of the neutron skin, *Nucl. Phys. A* **336**, 267 (1980).
- [39] X. Roca-Maza and N. Paar, Nuclear equation of state from ground and collective excited state properties of nuclei, *Prog. Part. Nucl. Phys.* **101**, 96 (2018).
- [40] Z. Z. Li, Y. F. Niu, and G. Colò, Toward a Unified Description of Isoscalar Giant Monopole Resonances in a Self-Consistent Quasiparticle-Vibration Coupling Approach, *Phys. Rev. Lett.* **131**, 082501 (2023).
- [41] M. Warda, X. Viñas, X. Roca-Maza, and M. Centelles, Neutron skin thickness in the droplet model with surface width dependence: Indications of softness of the nuclear symmetry energy, *Phys. Rev. C* **80**, 024316 (2009).
- [42] M. Centelles, X. Roca-Maza, X. Viñas, and M. Warda, Origin of the neutron skin thickness of  $^{208}\text{Pb}$  in nuclear mean-field models, *Phys. Rev. C* **82**, 054314 (2010).
- [43] J. Dobaczewski, H. Flocard, and J. Treiner, Hartree-Fock-Bogolyubov description of nuclei near the neutron drip line, *Nucl. Phys. A* **422**, 103 (1984).
- [44] E. Chabanat, P. Bonche, P. Haensel, J. Meyer, and R. Schaeffer, A Skyrme parametrization from subnuclear

- to neutron star densities Part II. Nuclei far from stabilities, *Nucl. Phys. A* **635**, 231 (1998).
- [45] J. C. Slater, A Simplification of the Hartree-Fock Method, *Phys. Rev.* **81**, 385 (1951).
- [46] M. V. Stoitsov, N. Schunck, M. Kortelainen, N. Michel, H. Nam, E. Olsen, J. Sarich, and S. Wild, Axially deformed solution of the Skyrme-Hartree-Fock-Bogoliubov equations using the transformed harmonic oscillator basis (II) HFBTHO v2.00d: A new version of the program, *Comput. Phys. Commun.* **184**, 1592 (2013).
- [47] T. Naito, T. Oishi, H. Sagawa, and Z. Wang, Comparative study on charge radii and their kinks at magic numbers, *Phys. Rev. C* **107**, 054307 (2023).
- [48] H. Sagawa, G. Colò, X. Roca-Maza, and Y. Niu, Collective excitations involving spin and isospin degrees of freedom, *Eur. Phys. J. A* **55**, 227 (2019).
- [49] J. Dobaczewski and J. Dudek, Time-odd components in the mean field of rotating superdeformed nuclei, *Phys. Rev. C* **52**, 1827 (1995).
- [50] X. Roca-Maza, G. Colò, and H. Sagawa, New Skyrme interaction with improved spin-isospin properties, *Phys. Rev. C* **86**, 031306 (2012).
- [51] N. Van Giai and H. Sagawa, Spin-isospin and pairing properties of modified Skyrme interactions, *Phys. Lett. B* **106**, 379 (1981).
- [52] J. Bartel, P. Quentin, M. Brack, C. Guet, and H.-B. Håkansson, Towards a better parametrisation of Skyrme-like effective forces: A critical study of the SkM force, *Nucl. Phys. A* **386**, 79 (1982).
- [53] S. Goriely, M. Samyn, J. M. Pearson, and M. Onsi, Further explorations of Skyrme-Hartree-Fock-Bogoliubov mass formulas. IV: Neutron-matter constraint, *Nucl. Phys. A* **750**, 425 (2005).
- [54] M. Kortelainen, T. Lesinski, J. Moré, W. Nazarewicz, J. Sarich, N. Schunck, M. V. Stoitsov, and S. Wild, Nuclear energy density optimization, *Phys. Rev. C* **82**, 024313 (2010).
- [55] M. Kortelainen, J. McDonnell, W. Nazarewicz, P.-G. Reinhard, J. Sarich, N. Schunck, M. V. Stoitsov, and S. M. Wild, Nuclear energy density optimization: Large deformations, *Phys. Rev. C* **85**, 024304 (2012).
- [56] M. Kortelainen, J. McDonnell, W. Nazarewicz, E. Olsen, P.-G. Reinhard, J. Sarich, N. Schunck, S. M. Wild, D. Davesne, J. Erler, and A. Pastore, Nuclear energy density optimization: Shell structure, *Phys. Rev. C* **89**, 054314 (2014).
- [57] X. Roca-Maza, M. Brenna, B. K. Agrawal, P. F. Bortignon, G. Colò, L.-G. Cao, N. Paar, and D. Vretenar, Giant quadrupole resonances in  $^{208}\text{Pb}$ , the nuclear symmetry energy, and the neutron skin thickness, *Phys. Rev. C* **87**, 034301 (2013).